Integration of temporal & spatial properties of dynamic functional connectivity based on two-directional two-dimensional principal component analysis for disease analysis

Feng Zhao[1], Ke Lv[1], Shixin Ye[1], Xiaobo Chen[1], Hongyu Chen[2], Sizhe Fan[3], Ning Mao[4] and Yande Ren[5]

[1] School of Computer Science and Technology, Shandong Technology and Business University, Yantai, China
[2] School Hospital, Shandong Technology and Business University, Yantai, China
[3] Canada Qingdao Secondary School (CQSS), Qingdao, China
[4] Department of Radiology, Yantai Yuhuangding Hospital, Yantai, China
[5] Department of Radiology, The Affiliated Hospital of Qingdao University, Qingdao, China

ABSTRACT

Dynamic functional connectivity, derived from resting-state functional magnetic resonance imaging (rs-fMRI), has emerged as a crucial instrument for investigating and supporting the diagnosis of neurological disorders. However, prevalent features of dynamic functional connectivity predominantly capture either temporal or spatial properties, such as mean and global efficiency, neglecting the significant information embedded in the fusion of spatial and temporal attributes. In addition, dynamic functional connectivity suffers from the problem of temporal mismatch, *i.e.*, the functional connectivity of different subjects at the same time point cannot be matched. To address these problems, this article introduces a novel feature extraction framework grounded in two-directional two-dimensional principal component analysis. This framework is designed to extract features that integrate both spatial and temporal properties of dynamic functional connectivity. Additionally, we propose to use Fourier transform to extract temporal-invariance properties contained in dynamic functional connectivity. Experimental findings underscore the superior performance of features extracted by this framework in classification experiments compared to features capturing individual properties.

Subjects Neuroscience, Neurology, Psychiatry and Psychology, Radiology and Medical Imaging, Computational Science
Keywords Dynamic functional connectivity, Spatial and temporal properties

Submitted 26 October 2023
Accepted 19 February 2024
Published 9 April 2024

Corresponding author
Hongyu Chen,
chenhongyu1016@163.com

Academic editor
Feng Liu

Additional Information and Declarations can be found on page 15

DOI **10.7717/peerj.17078**

INTRODUCTION

The human brain is a complex functional system that is artificially divided into different brain regions. Each brain region has a different primary function and they work together to accomplish complex tasks. An in-depth study of the interactions between brain regions can reveal the operating mechanisms of the brain and lay the foundation for the discovery of the pathogenesis of brain diseases (*Angermann et al., 2022*; *Bai et al., 2009*; *Chopade*

How to cite this article Zhao F, Lv K, Ye S, Chen X, Chen H, Fan S, Mao N, Ren Y. 2024. Integration of temporal & spatial properties of dynamic functional connectivity based on two-directional two-dimensional principal component analysis for disease analysis. *PeerJ* **12**:e17078 http://doi.org/10.7717/peerj.17078

et al., 2023). In order to study the correlations between different brain regions of the brain as they work, a large number of studies have used resting-state functional magnetic resonance (rs-fMRI) to construct functional connectivity (FN) between different brain regions, which characterizes the interactions between different brain regions (*Damaraju et al., 2014*; *Dawson, Rieder & Johnson, 2023*; *Farah et al., 2020*; *Gao et al., 2022*; *Grandjean et al., 2023*). Currently, functional connectivity is now a key tool to help further our understanding and aid in the diagnosis of neurological disorders such as Parkinson's disease and autism (*Holz et al., 2023*; *Huber et al., 2021*; *Hutchison et al., 2013*; *Kazeminejad & Sotero, 2019*).

Functional connectivity is generally categorized into two main groups: (1) static functional connectivity, which assumes that rs-fMRI is constant throughout the recording period and does not change over time. Higher-order brain networks based on static functional connectivity achieve good results in assisting the diagnosis of neurological diseases (*Kumar & Aravind, 2010*; *Ladwig et al., 2022*; *Lawrence et al., 2020*; *Li et al., 2020*); (2) dynamic functional connectivity (DFC), which characterizes the dynamics of functional connectivity over time, and is generally derived from functional connectivity time series by the ''sliding window'' method. Dynamic functional connectivity has better performance on classification tasks because it contains time-varying information (*Liu et al., 2020*; *Liu et al., 2019*; *Long et al., 2020*; *Lu et al., 2019*; *Lurie et al., 2020*; *Matson & Nebel-Schwalm, 2007*). On the one hand the dynamics of functional connectivity over time can be referred to as the temporal properties of dynamic functional connectivity. On the other hand, the brain as a complex functional system has not only interactions between regions of interest (ROIs), but also complex spatial relationships between different functional connections, which reflect the spatial properties of functional connections.

Although dynamic functional connectivity includes both temporal and spatial properties, researchers have mostly analyzed one aspect of a single property. For example, for temporal properties, most studies use statistical methods to count the minimum, maximum, mean, standard deviation, root mean square, *etc.*, of the time series of dynamic functional connectivity (*Ni et al., 2014*; *Olczyk et al., 2022*; *Pang et al., 2022*). For spatial properties, most researchers have represented different functional brain regions and their connections as a brain network, and then statistically analyzed the characteristic path lengths, global efficiencies, and clustering coefficients of this network (*Park et al., 2020*; *Qiu et al., 2014*; *Razzak et al., 2020*). Few studies have been conducted to extract and analyze features that integrate both temporal and spatial properties of dynamic functional connectivity (*Ricaud et al., 2019*). It can be reasonably assumed that features combining complementary temporal and spatial properties can provide more critical information for brain disease research and more differential information for classifiers, which in turn improves the correctness of the diagnosis of neurological disorders and the diagnostic efficiency of doctors. Therefore, a framework is needed to extract features that simultaneously contain the temporal and spatial properties of dynamic functional connectivity.

Based on the above analysis, we propose a new feature extraction framework based on two-directional two-dimensional principal component analysis ($(2D)^2$PCA) (*Royer et al., 2022*; *Sadat & Joye, 2020*; *Shen et al., 2023*), which is capable of extracting features that

integrate both temporal and spatial characteristics of dynamic functional connectivity. In this framework, we utilize the $(2D)^2$PCA function that can fully consider the properties of the matrix in both directions while eliminating noise, $(2D)^2$PCA is used to simultaneously consider the relationship between the temporal and spatial orientations of the dynamic functional connectivity, and thus integrates the properties in both directions. To the best of our knowledge, there is no $(2D)^2$PCA based feature extraction method for dynamic functional connectivity to extract features. In contrast to previous feature extraction methods that only capture structural information in a single direction, the proposed $(2D)^2$PCA based feature extraction method can simultaneously integrate features in both directions.

In addition, dynamic functional connectivity suffers from the problem of sensitive to the chronological order of its subnetworks, which limits its use in comparative studies (*Shi et al., 2019*). The Fourier transform has been widely used in the field of communications, acoustics and optics, where it converts signals that are difficult to analyze in the time domain into a frequency domain representation and then goes on to analyze them (*Starck et al., 2013*; *Sun et al., 2022*; *Sun et al., 2019*; *Valentine, Al-Mualem & Baiz, 2021*; *Valsasina et al., 2019*). Inspired by the Fourier transform function, we propose to use the Fourier transform to solve the problem. In the feature extraction framework, the time series of different functional connections are converted from time domain to frequency domain representation by Fourier transform. By comparing the information on the same frequency instead of comparing the information on the same time point, the impact of temporal mismatch on to the dynamic functional connectivity comparison study is mitigated.

In order to verify that the features extracted by the framework have better separability, we trained classifiers using the extracted features for subsequent adjunctive diagnosis of neurological disorders and conducted experiments in two brain disease classification tasks. The experimental results show that the features extracted by the framework perform better in disease-assisted diagnosis than those extracted by feature extraction methods that only include temporal or spatial unidirectional features, and the Fourier transform mitigates the problem of dynamic functional connectivity being sensitive to the temporal order of its subnetworks. In addition, the extracted features show a performance improvement over the comparison methods on both classification tasks, and it can be found that our proposed framework is aiding in the diagnosis of neurological disorders, and not only for a particular disease.

In summary, there are two parts of contribution in this article: (1) proposing a new feature extraction framework for extracting features that integrate temporal and spatial properties of dynamic functional connectivity; (2) utilizing the Fourier transform method to capture dynamic functional connectivity properties without performing chronological time matching. The framework has promising applications in the detection, prevention and prognostic assessment of brain diseases, and the abnormal functional connectivity and brain regions of brain disease patients identified in the article can provide new perspectives for subsequent research.

MATERIALS AND DATA PREPROCESSING

Subjects

The rs-fMRI data of 45 autism spectrum disorders (ASD) patients and 47 healthy controls (HC) groups were scanned using a 3-T Siemens Allegra scanner at the NYU Langone Medical Center. Due to the difference in medical device, collection protocol, *etc* to mitigate data heterogeneity, scans were exclusively considered from 45 individuals diagnosed with ASD and 47 individuals within the age range of 7 to 15 years. The imaging was conducted at NYU Langone Medical Center. All subjects under consideration exhibited minimal head movement, with displacement <1.5 mm or angular rotation <1.5° in any of the three directions. The ASD subjects were diagnosed according to the autism criteria in the Diagnostic and Statistical Manual of Mental Disorders (4th Edition, Text Revised) (DSM-IV-TR) (*American Psychiatric Association, 2000*). For more details of the data collection, exclusion criteria, and scan parameters, please visit the ABIDE website. The main scanning parameters used in this dataset include the flip angle = 90, 33 slices, TR/TE = 2,000/15 ms, 180 volumes, and voxel thickness = 4 mm.

The rs-fMRI data of 52 end-stage renal disease (ESRD) patients and 49 HC groups were scanned using GE Signa HDX 3.0T MRI equipment at hospital of Qingdao University. Inclusion criteria for the ESRD group: (1) Diagnosed by the Affiliated Hospital of Qingdao University as Chronic Kidney Disease Stage 5, glomerular filtration rate less than 15 ml $\cdot \min^{-1} \cdot \left(1.73\ m^2\right)^{-1}$. (2) Age 18–70 years old; (3) No contraindications to magnetic resonance examination and claustrophobia. Exclusion criteria: (1) history of severe traumatic brain injury; (2) intracranial organic pathology, intracranial organic disease, such as tumour, infarction, haemorrhage, *etc*.; (3) cerebrovascular disease, such as cerebral arteriovenous malformation, smoky disease, *etc*. and smog disease; (4) history of mental illness; and (5) history of substance abuse (drug ethanol or cigarettes); (6) hypertension, diabetes mellitus, coronary artery disease, heart failure, liver and kidney failure, *etc*. failure, liver or kidney failure, and other serious systemic diseases; (7) incompatibility with the test subjects who are incompatible with the test or unable to effectively complete the MRI scan. The scan parameters are TR = 3,000 ms, TE = 40 ms, FA = 90°, 25 slices, thickness = 5 mm, gap = 0 mm, matrix size = 96×96 and FOV = 24 cm × 24 cm.

Data preprocessing

Data preprocessing is performed for all rs-fMRI data by using a standard pipeline, including time correction, head motion correction, spatial normalization and smoothing using MATLAB's DPABI toolbox. Specifically, (1) conversion of data format; (2) removal of data from the first 10 sampling points for each subject in order to exclude the effects of initial magnetic field instability and the subject's initial emotional instability; (3) correction of time layer, head motion. Subjects with excessive head movements are excluded; (4) spatial normalization in terms of MNI standard space with the resolution of 3 × 3 × 3 mm^2; (5) ventricle signals, cerebrospinal fluid signal and white matter signal were regressed out as nuisance signals; (6) to filter out various physiological noises to reduce the effects of low-frequency linear drift and physiological noise, the data were processed to remove linear trends and band-pass filtered (0.01−0.08 Hz).

In this experiment, after data pre-processing, the brain was divided into 116 brain regions for each subject according to the AAL template, and the average of the BOLD signal of all voxels in each brain region was calculated to obtain the average time series of the 116 brain regions.

METHODS

In this section, we first introduce DFC construction, the Fourier transform and $(2D)^2$PCA technology, and then present the details of the construction of the framework proposed in this article.

Construction of DFC

For each subject, let $z_i = (z_{i1}, z_{i2}, \ldots, z_{iN})$ $(i = 1, 2, \ldots, 116)$ denotes the average rs-fMRI time series of the ith brain region, where N denotes the number of image time points. Dynamic FC is implemented using a sliding window approach, assuming that the length of the sliding window is T, and the step length between every two adjacent windows is S. Then the time series of length N is divided into K partially overlapping subseries with each other, where $K = \frac{[(N-T)]}{S} + 1$.

Letting $z_i(k) = [z_{i1}(k), z_{i2}(k), \ldots, z_{iT}(k)]\,(k = 1, 2, \ldots, K)$ denotes the kth time subseries of z_i, then just need to list all sliding windows of FC. FC is often modeled as a FC network (FCN), with each brain ROI as a node in the network, and the strength of FC between a pair of brain ROIs as an edge. The FCN of the kth time subseries can be generated by a symmetric submatrix D(k), defined as:

$$D(k) = [\rho_{ij}(k)]_{1 \le i,j \le K} \tag{1}$$

where $\rho_{ij}(k)$ denotes the Pearson's correlation between the average time subseries $z_i(k)$ and $z_j(k)$, defined as:

$$\rho_{ij}(k) = \frac{\sum_{t=1}^{T} \left(z_{it}(k) - \overline{z_i(k)}\right)\left(z_{jt}(k) - \overline{z_j(k)}\right)}{\sqrt{\sum_{t=1}^{T} \left(z_{it}(k) - \overline{z_i(k)}\right)^2} \sqrt{\sum_{t=1}^{T} \left(z_{jt}(k) - \overline{z_j(k)}\right)^2}} \tag{2}$$

where $\overline{z_i(k)}$ and $\overline{z_j(k)}$ denote average value of the average time subseries $z_i(k)$ and $z_j(k)$. The submatrix series $\{D(k)\}_{k=1}^{K}$ can describe the temporal change of the connectivity strength for all ROI pairs.

The Fourier transform

Discrete Fourier Transform, as a mathematical tools, is commonly used in signal processing. The Discrete Fourier Transform can convert a signal into a linear combination of a set of sinusoidal functions of different frequencies, which have the property of being easy to implement and observe.

The Discrete Fourier Transform of vector $x(k), k = \{1, 2, \ldots, K\}$ is defined as:

$$f(u) = \sum_{k=1}^{K} x(k)\, W_K^{(k-1)(u-1)} \tag{3}$$

where u denote the frequency-domain pixel coordinate of C_r, $u = \{1, 2, \ldots, K\}$, W_K is defined as:

$$W_K = e^{\frac{-2\pi i}{K}}. \tag{4}$$

$(2D)^2$ PCA

$(2D)^2$PCA is a matrix feature extraction technique based on two-dimensional principal component analysis (2DPCA). 2DPCA can extract whole-matrix features by finding optimal projection directions from the covariance matrix. First introduce how 2DPCA learns an optimal projection matrix reflecting the information between rows of matrixes. Letting $A \in R^{m \times n}$ be a matrix, $X \in R^{n \times d}$ be a projection matrix with n projection directions. Projecting A onto X to obtain the matrix $Y = AX$. Suppose that there are M training matrixes, denoted by $A_k (k = 1, 2, \ldots, M)$, and denote the covariance matrix as:

$$X = \frac{1}{M} \sum_{k}^{M} \left(A_k - \overline{A}\right)^T \left(A_k - \overline{A}\right) \tag{5}$$

where $\overline{A}$ be denoted as:

$$\overline{A} = \frac{1}{M} \sum_{k}^{M} A_k \tag{6}$$

The optimal value for the projection matrix X is composed by the vectors $X_1, X_2, \ldots, X_d$ of G corresponding to the d largest eigenvalues. The value of d can be controlled as follows:

$$\frac{\sum_{i=1}^{d} \lambda_i}{\sum_{i=1}^{n} \lambda_i} \geq \theta \tag{7}$$

where $\lambda = \{\lambda_1, \lambda_2, \ldots, \lambda_n\}$ is a sequence of eigenvalues in ascending order for G and θ is a pre-set threshold.

2DPCA also can learn an optimal matrix Z reflecting the information between columns, and then projects A onto Z to obtain the matrix $B = Z^T A$, and denote the covariance matrix as:

$$Z = \frac{1}{M} \sum_{k}^{M} \left(A_k - \overline{A}\right) \left(A_k - \overline{A}\right)^T \tag{8}$$

$(2D)^2 PCA$ is a way to simultaneously use the projection matrices X and Z. Projecting A onto X and Z, yielding a matrix C:

$$C = Z^T A X \tag{9}$$

The matrix C in Eq. (9) is the matrix after projection.

Comparison methods

In this section we describe two comparison methods used in subsequent experiments: the central moment method and the topological index method.

The central moment method

The feature extraction method based on the central moment method is a feature extraction method designed for retaining the temporal information of dynamic functional connections. As follows, $\rho_{ij}(k)$ is calculated according to Eq. (2), and then dth order central-moment $m_{ij}(d)$ of $\rho_{ij}(k)$ is calculated:

$$m_{ij}(d) = \sqrt[d]{\frac{\sum_{k=1}^{K}\left[\rho_{ij}(k) - \overline{\rho}_{ij}\right]^d}{K}} \ (d = 1, 2, \ldots, D) \tag{10}$$

where D denotes the highest order, $\overline{\rho}_{ij}$ is the mean of $\rho_{ij}(k)(k = 1, 2, \ldots, \mathrm{K})$.

Different central moment features represent different information about the dynamic functional connectivity in the time direction, and it represents different discriminatory power, so the order of the central moment should be carefully chosen. d is a parameter in the central moment feature framework that needs to be adjusted in subsequent training. Finally, the selected features are fed into the SVM classifier.

The topological index method

Converting dynamic functional connectivity to topology. Specifically, first define the threshold value T and ignore this functional connection by changing the value $\rho_{ij}(k) < T$ to 0. Then the topology is constructed by retaining the weights of the edges of $\rho_{ij}(k) \geq T$ or changing them to 1. We have empirically changed the top 20 per cent of weights to 1 and the rest to 0 (*Van Den Heuvel & Pol, 2010*). The calculated topological index consisted of measures of segregation (Clustering Coefficient, Transitivity), integration (Characteristic Path Length, Efficiency), and centrality (Betweenness centrality, within module degree Z-score, Participation coefficient) of the brain network. Formulas for each metric are presented in the article (*Wang, Zhang & Qiao, 2023*). The selected features are fed into the SVM classifier.

Construction of the proposed framework

In this subsection, we describe the proposed framework building process in detail. Figure 1 depicts the main steps of the feature extraction framework, and it can be seen that there are four main steps: (1) Construction of the dynamic network. (2) Construction of the new network. (3) $(2D)^2PCA$ learns the best projection matrix. (4) Projecting the new network and selecting features.

Specifically, we first construct the DFC $\{D(k)\}_{k=1}^{K}$ on the continuous rs-fMRI time series by the sliding-window strategy. Then in order to retain both temporal and spatial dynamic information, we transform the 3D DFC into a 2D new network, so that the spatial and temporal information to be stored in the row and column structure of the new network.

Figure 2 illustrates the process of new network construction. For each subject, we transform the submatrix series $\{D(k)\}_{k=1}^{K}$ into a matrix $A \in R^{M*K}$, where M denotes the number of upper triangular elements of matrix $D(k)$. The upper triangular elements of matrix $D(k)$ are pulled into a column vector as the kth column of matrix A. Each row of matrix A reflects the change of each functional connectivity series $\left\{\rho_{ij}(k)\right\}_{k=1}^{K}$ over time. To solve the problem that the correspondence of dynamic FC subnetworks from the same

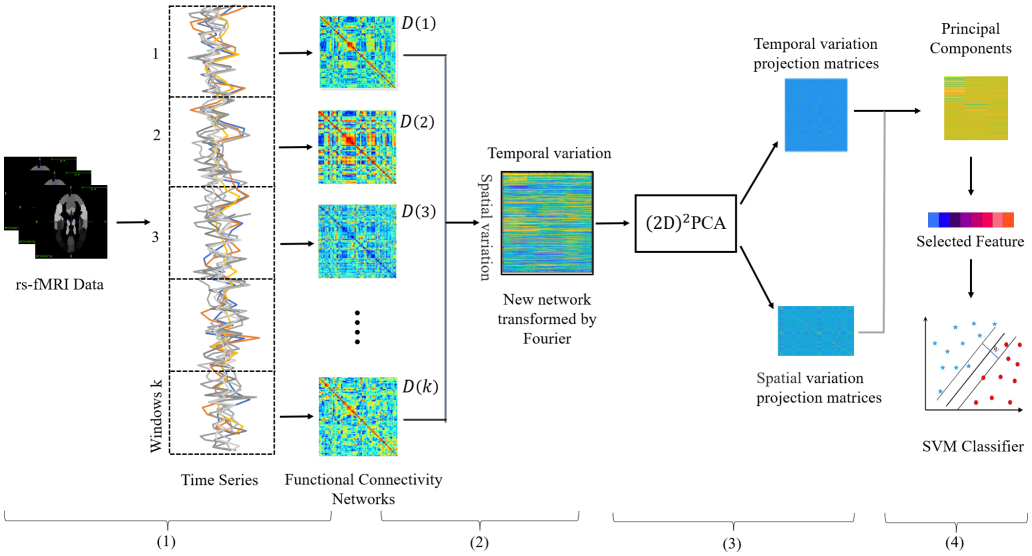

Figure 1 Illustration of the proposed feature extraction framework integrating both temporal and spatial properties of DFCs. Including (1) rs-fMRI image preprocessing and networks construction, (2) doing Fourier transform and new network construction, (3) obtaining the best projection matrix in both directions by $(2D)^2$ PCA, (4) Selecting features and training SVM classifier.

Full-size DOI: 10.7717/peerj.17078/fig-1

window of different subjects cannot be established, we convert the time series $\{\rho_{ij}(k)\}_{k=1}^{K}$ from the time domain to the frequency domain by Fourier transform, which is calculated by Eq. (3). After transformation, the transformation of functional connectivity with time is represented by a linear combination of 'trigonometric functions of different frequencies, so we can analyze the problem from a new perspective, which eliminates the problem of time not corresponding.

Furthermore, we use $(2D)^2$PCA to learn the best projection matrix, which is calculated by Eqs. (5) and (8). The new network is projected by Eq. (9) with the optimal projection matrix to select features that integrate spatial and temporal properties of the new network. $(2D)^2$PCA is widely used for image matrix dimensionality reduction in face recognition and palmprint recognition, which can learn two optimal matrixes from a set of training matrixes reflecting information between rows and between columns of training matrixes, so $(2D)^2$PCA can integrate properties in both directions.

Finally, the features extracted by $(2D)^2$PCA will have high dimensionality, so an effective feature selection method is conducive to accurate diagnosis. For dichotomous classification tasks, t-test can be effective in selecting significantly different features between subjects and healthy controls. Therefore, we use a t-test to select the features with p-values less than a certain threshold value.

EXPERIMENTS AND RESULTS

This section contains three sub-chapters: methods for comparison, experimental setting and classification performance.

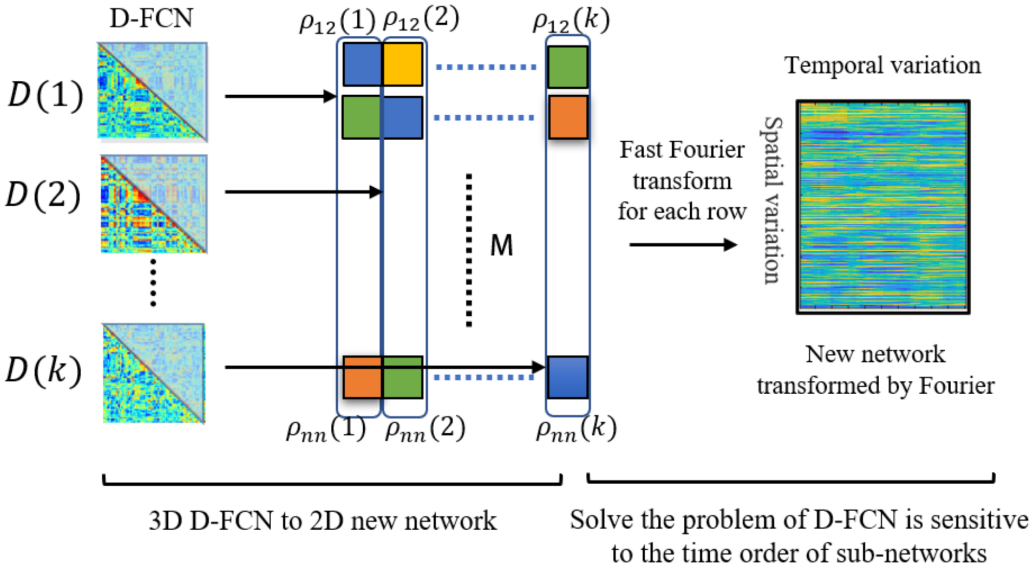

Figure 2 **Illustration the process of new network construction.** p_{ij} (k) denotes the value of the i-th row and j-th column of functional connectivity network $D(k)$. M denotes the number of upper triangular elements of functional connectivity networks D.

Full-size DOI: 10.7717/peerj.17078/fig-2

Methods for comparison

We first compare our proposed method with the central moment method (denoted as Central). In the central moment method, the Pearson correlation between ROI based on the time series of each window is first computed, then the brain networks between ROI are constructed, and the multistep central moment of the brain networks of all the windows solved are used as features for the classification task. Then we compare our proposed method with the method that use topological index of functional connectivity to classify (defined as T-index). In the topological index method, the topology is generated by retaining as nodes the functional connections in the dynamic functions that are greater than a certain threshold, and then the topological index of the topology is derived for binary classification.

Moreover, we compare our proposed method with two methods for extracting unidirectional information using two-dimensional principal component analysis (2DPCA) (*Wang, Wang & Yan, 2018*; *Wee et al., 2016*; *Xu et al., 2019*), which include (1) the method using 2DPCA in the temporal direction (denoted as Fourier-temporal), and (2) the method using 2DPCA in the spatial direction (denoted as Fourier-spatial). In this way, it is demonstrated that $(2D)^2$PCA can integrate temporal and spatial information improves the performance of classification. It is worth noting that both methods use the Fourier transform to eliminate the effects of time mismatch.

In order to demonstrate that the Fourier transform can play a role in eliminating the time mismatch problem. We also compare our proposed method with that of $(2D)^2$PCA which does not use Fourier transform (denoted as Temporal-spatial). All the methods use

the same T-test as the proposed method for feature selection, and then the features are fed into a SVM classifier for classification.

Experimental setting

In the experiment, we constructed two classification tasks, including (1) the classification task for autism spectrum disorder (ASD) and normal control group (NC), and (2) the classification task for end-stage renal disease (ESRD) and NC. We used six evaluation indexes, namely, classification accuracy (ACC), true positive rate (TPR), true negative rate (TNR), positive predictive value (PPV), negative predictive value (NPV), and F1 score, to comprehensively evaluate the advantages and disadvantages of the parameters and the classification effect of the methods. Considering that the number of samples used in the experiments is more than 50 and the parameters such as sliding window length, sliding step size, information content thresholds for temporal and spatial directions, and p-value thresholds need to be adjusted in the feature extraction framework proposed in this article. After referring to the relevant literature (*Shi et al., 2019*), we selected the ten-fold cross-validation method, which appears in the literature, and did not choose the leave-one-out method, which is more computationally intensive. To avoid possible errors in the experiments, the whole ten-fold cross-validation was repeated 10 times, dividing the samples randomly each time. Finally, the average of the 10 times of recognition accuracy was used as the final accuracy.

In the construction of the network, in order to avoid erroneous experimental results with arbitrarily determined window width and step size, we constructed brain networks with different window widths and step sizes, window width parameter $T \in [20, 30, 40, 50, 60]$ and sliding step size $S \in [2, 4, 6, 8, 10]$. Studies have shown that window width and step size in this range produce robust results in image acquisitions and topological properties of brain networks. We take the DFC derived from all the different parameters and take the average value as the final DFC. In the feature selection phase, we choose features with statistical significance $p < 0.01$. After that, the features are fed into a SVM classifier for training and classification, and the six metrics mentioned in the previous paragraph are calculated (*Yang et al., 2022*; *Yao, Becker & Kendrick, 2021*).

Classification performance

Table 1 summarizes the classification performance of each of the six methods in the two classification tasks. From Table 1, we can see that our proposed method performs better than comparison methods. For example, the proposed method acc achieves 88.1% and 76.1% in the two classification tasks and the highest accuracy of the comparison method is at 86.1% and 72.8%. Table 1 shows that the method integrating temporal and spatial information of the network performs better than the method using one attribute alone, which implies that the temporal and spatial information are two complementary pieces of information, so integrating the brain through $(2D)^2$PCA network's two kinds of information can further improve the classification performance.

In addition, we could observe that, from Table 1, that using Fourier transform to transform the DFC from the time domain to the frequency domain has a higher

Table 1 Results of five methods on two classification tasks.

Task	Method	ACC (%)	TPR (%)	TNR (%)	PPV (%)	NPV (%)	F1 (%)
NC *vs.* ESRD	Fourier-spatial	85.2	88.9	81.5	84.3	89.6	85.8
	Fourier-temporal	85.1	88.4	81.7	83.9	87.1	86.0
	Temporal-spatial	86.1	84.6	87.8	88.0	84.0	86.3
	T-index	82.2	80.8	83.7	84.0	80.4	82.4
	Central	85.1	82.4	87.7	87.6	83.5	84.7
	Proposed	**88.1**	**92.4**	84.0	86.9	**91.8**	**89.0**
NC *vs.* ASD	Fourier-spatial	71.7	66.7	76.7	73.2	70.1	69.8
	Fourier-temporal	70.1	68.9	72.3	70.0	70.1	69.7
	Temporal-spatial	72.8	71.1	74.5	72.7	72.9	71.9
	T-index	68.3	67.3	69.4	70.0	66.7	68.6
	Central	68.5	64.4	72.3	69.1	68.0	66.7
	Proposed	**76.1**	**73.3**	**78.7**	**76.7**	**75.5**	**75.0**

Notes.
Values highlighted in bold show best results in the classification task.

classification accuracy than the method that does not use Fourier transform, so we can think that Fourier transform can eliminate the effect of time mismatch to a certain extent and bring better classification performance.

In the process of constructing the dynamic brain network, we used the "sliding window" strategy, so there are two hyperparameters, window width and step size, and we subsequently evaluated the effect of hyperparameters on the classification performance in the classification experiments of nephropathic and normal human beings. Figure 3 shows the effect of different hyperparameters on the classification performance in the four methods, namely Fourier-spatial, Fourier-temporal, Central and our proposed method. It can be concluded that there is an effect of hyperparameters on the classification performance, and our proposed method has more stable and higher classification performance on different combinations of hyperparameters, and has the highest classification accuracy of 88.1% when $T = 50$ and $S = 8$.

DISCUSSION

Numerous studies have shown significant changes in dynamic functional connectivity in patients with brain diseases. Studying changes in the brain's dynamic connectivity network may contribute to a better understanding of brain diseases and help with early prevention and later treatment. Currently, the study of dynamic functional connectivity in patients with brain diseases is limited to a single feature of a single characteristic. These features do not integrate the temporal and spatial properties of dynamic functional connectivity. In this article, we propose a feature extraction framework that integrates both temporal and spatial bidirectional information of dynamic functional connectivity. Experimentally, it is found that the features extracted by this framework are helpful for the assisted diagnosis of brain diseases, compared to feature extraction methods that contain only temporal direction information.

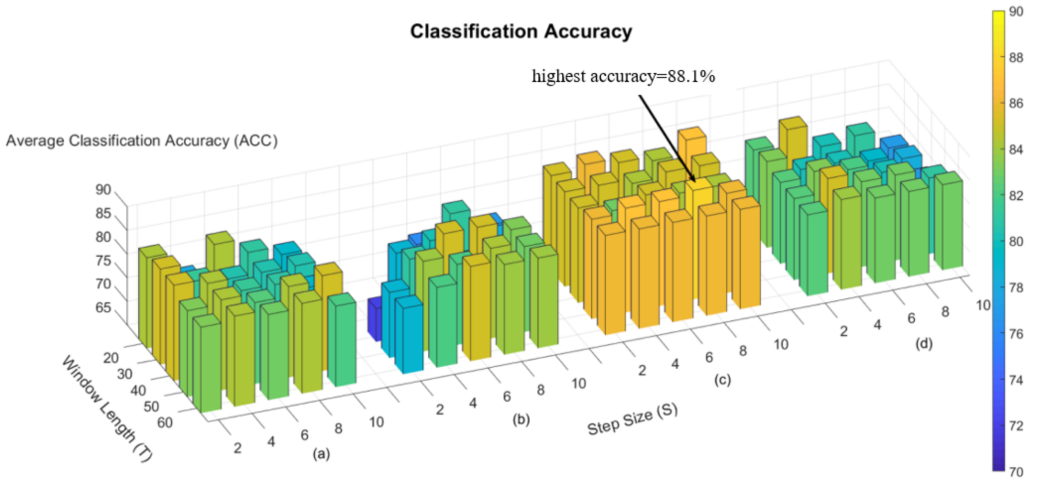

Figure 3 Accuracy of four methods in the task for ESRD and NC. (A) ACC of Fourier-spatial. (B) ACC of Fourier-temporal. (C) ACC of our proposed method. (D) ACC of Central.
Full-size DOI: 10.7717/peerj.17078/fig-3

In order to verify that the features extracted from our proposed framework perform better on the classification task, we used them to train classifiers and make predictions. Considering the two current problems of dynamic functional connectivity mentioned in the article, which may be common to most neurological disorders. In order to validate that our proposed framework has a role to play in a wide range of neurological disorders, we conducted classification experiments on two different neurological disorders datasets. The experiments revealed that the classification performance was improved to some extent on both classification tasks. On the classification task of ASD and NC, the classification performance is improved more, probably because the diagnosis of ASD patients relies more on the combination of temporal and spatial information.

Experiments show that our proposed method has better classification performance than both the central moment method and the local variable method. This suggests that both temporal and spatial information of dynamic functional connectivity can provide support for classification, and combining complementary spatial and temporal information is responsible for the improved classification performance. The classification performance of using 2DPCA for feature extraction framework in one direction is lower than that of our proposed framework, which also confirms that combining complementary spatial and temporal information can improve the classification performance. Also, through experiments we can find that using Fourier transform can improve the classification performance. This is because the Fourier change converts dynamic functional connectivity to frequency domain information, and replaces the way of comparing information at the same time point with the way of comparing information at the same frequency, which avoids the problem of mismatch of information at the same time point and improves the classification performance.

We investigate the important features extracted through our proposed method to discover the brain regions most likely to be abnormal in ESRD patients and autistic

Table 2 Abbreviations and name of ROIs selected for the experiment.

	Abbreviation	ROI name	Abbreviation	ROI name
ESRD	INS	Insula	SMA	Supplementary motor area
	TPOsup	Temporal pole: superior temporal gyrus	ROL	Rolandic operculum
	PoCG	Postcentral gyrus	IPL	Inferior parietal, but supramarginal and angular gyri
	STG	Superior temporal gyrus	PCUN	Precuneus
	CAL	Calcarine fissure and surrounding cortex	ACG	Anterior cingulate and paracingulate gyri
	SFGmed	Superior frontal gyrus, medial		
ASD	ITG	Inferior temporal	PCUN	Precuneus
	PHG	Parahippocampal gyrus	TPOmid	Temporal pole: middle temporal gyrus
	REC	Rectus gyrus	TPOsup	Temporal pole: superior temporal gyrus
	PCG	Posterior cingulate gyrus	INS	Insula
	SMA	Supplementary motor area	ORBsupmed	Orbitofrontal cortex (medial)

patients. Each selected feature, contains both temporal and spatial information, and there exists an element that contributes the most information to that feature in both spatial and temporal directions. In the spatial direction, the element that contributes the most information represents the functional connectivity between two brain regions that we believe are most likely to have abnormalities. For the categorization experiments, the features selected in each cross-validation experiment were different, so we chose features with a p-value of less than 0.01 and appearing in each cross-over experiment. The ROIs most likely to be abnormal in patients with end-stage renal disease and autism are given in Table 2, Figs. 4 and 5 depicts these functional connections and the corresponding brain regions, where L and R denote the left and right hemispheres of the brain.

From Fig. 4, we find that the precuneus and temporal lobes dominate among the brain regions most associated with ESRD. Of these, the precuneus is associated with many high-level cognitive functions, such as situational memory, self-related information processing, and various aspects of consciousness, and abnormalities in the precuneus may contribute to the increased risk of cognitive impairment in ESRD patients. The temporal lobe is primarily responsible for language function and auditory perception, may be associated with decreased communication skills in ESRD patients (*Ye et al., 2023*; *Yu et al., 2020*; *Zhang et al., 2011*). From Fig. 5, it can be concluded that most of the brain regions associated with ASD are related to motor coordination and emotional expression, such as the posterior cingulate gyrus (*Zhang & Small, 2006*; *Zhao et al., 2020*; *Zhou et al., 2019*; *Zou et al., 2021*).

This study needs to consider the following limitations. (1) the relatively small sample size in this study will affect the stability of the experimental results. In future studies we will use a larger sample size to verify the correctness of our conclusions. (2) The scan period of rs-fMRI is short, and the dynamic characteristics are not reflected enough. A longer scan period can better reflect the change of functional connectivity over time, which may be crucial for future studies of dynamic functional connectivity. (3) The eigenvalues extracted

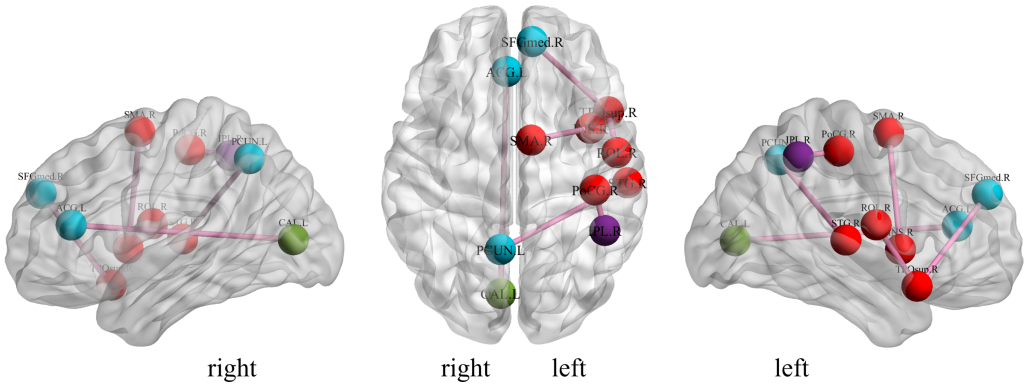

Figure 4 **Diagrammatic representation of the relevant functional connections of important features in ESRD.**

Full-size DOI: 10.7717/peerj.17078/fig-4

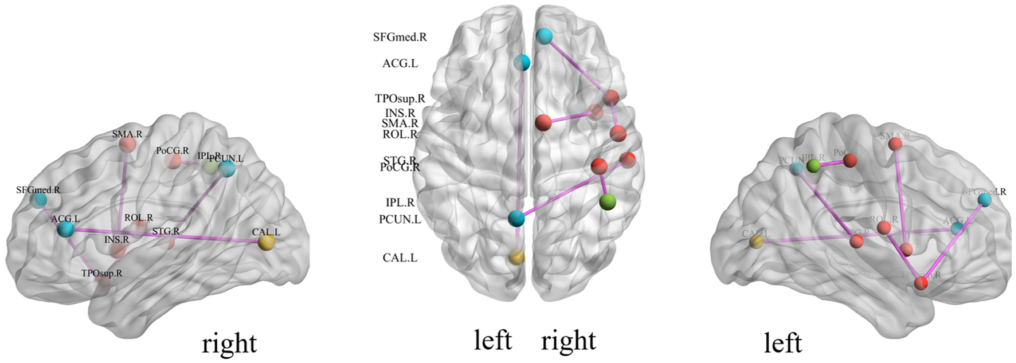

Figure 5 **Diagrammatic representation of the relevant functional connections of important features in ASD.**

Full-size DOI: 10.7717/peerj.17078/fig-5

by the framework are not given a specific meaning and cannot reflect the relevant changes directly through the eigenvalues.

CONCLUSION

In this article, we propose a feature extraction framework based on $(2D)^2$PCA that integrates both temporal and spatial properties of dynamic functional connectivity. The framework involves constructing the dynamic connectivity network using a sliding window strategy, addressing the sensitivity of dynamic functional networks to the order of subnetworks through Fourier transform, and leveraging $(2D)^2$PCA to integrate temporal and spatial information of dynamic functional connectivity. Experimental results demonstrate the complementary effects of considering both temporal and spatial orientations in improving feature extraction performance. These findings provide novel insights into the pathophysiological mechanisms underlying cognitive deficits from a dynamic functional connectivity perspective.

ADDITIONAL INFORMATION AND DECLARATIONS

Funding

This work was supported by the National Natural Science Foundation of China (62176140, 82001775, 61972235, 61976124, 61873117, 61976125) and the Central Guidance on Local Science and Technology Development Fund of Shandong Province (YDZX2022093). There was no additional external funding received for this study. The funders had no role in study design, data collection and analysis, decision to publish, or preparation of the manuscript.

Grant Disclosures

The following grant information was disclosed by the authors:
National Natural Science Foundation of China: 62176140, 82001775, 61972235, 61976124, 61873117, 61976125.
Central Guidance on Local Science and Technology Development Fund of Shandong Province: YDZX2022093.

Competing Interests

The authors declare there are no competing interests.

Author Contributions

- Feng Zhao conceived and designed the experiments, performed the experiments, analyzed the data, prepared figures and/or tables, authored or reviewed drafts of the article, and approved the final draft.
- Ke Lv performed the experiments, analyzed the data, prepared figures and/or tables, authored or reviewed drafts of the article, and approved the final draft.
- Shixin Ye analyzed the data, authored or reviewed drafts of the article, and approved the final draft.
- Xiaobo Chen analyzed the data, authored or reviewed drafts of the article, and approved the final draft.
- Hongyu Chen analyzed the data, authored or reviewed drafts of the article, and approved the final draft.
- Sizhe Fan analyzed the data, authored or reviewed drafts of the article, and approved the final draft.
- Ning Mao analyzed the data, authored or reviewed drafts of the article, and approved the final draft.
- Yande Ren analyzed the data, authored or reviewed drafts of the article, and approved the final draft.

Data Availability

The following information was supplied regarding data availability:

The code is available at GitHub and Zenodo:

- https://github.com/LvshanD/Code/tree/papercode
- Lv. (2023). code. Zenodo. https://doi.org/10.5281/zenodo.10443810

The Autism Brain Imaging Data Exchange (ABIDE) database is available at: http://fcon_1000.projects.nitrc.org/indi/abide/abide_I.html.

The functional connectivity raw data for the experimental patients with end-stage renal disease is available in the Supplemental File.

Supplemental Information

Supplemental information for this article can be found online at http://dx.doi.org/10.7717/peerj.17078#supplemental-information.

REFERENCES

American Psychiatric Association. 2000. Diagnostic and statistical manual of mental disorders. Text revision, 2000. Washington, D.C.: American Psychiatric Association.

Angermann S, Günthner R, Hanssen H, Lorenz G, Braunisch MC, Steubl D, Matschkal J, Kemmner S, Hausinger R, Block Z. 2022. Cognitive impairment and microvascular function in end-stage renal disease. *International Journal of Methods in Psychiatric Research* **31**:e1909 DOI 10.1002/mpr.1909.

Bai F, Zhang Z, Watson DR, Yu H, Shi Y, Yuan Y, Zang Y, Zhu C, Qian Y. 2009. Abnormal functional connectivity of hippocampus during episodic memory retrieval processing network in amnestic mild cognitive impairment. *Biological Psychiatry* **65**:951–958 DOI 10.1016/j.biopsych.2008.10.017.

Chopade P, Chopade N, Zhao Z, Mitragotri S, Liao R, Chandran Suja V. 2023. Alzheimer's and Parkinson's disease therapies in the clinic. *Bioengineering & Translational Medicine* **8**:e10367 DOI 10.1002/btm2.10367.

Damaraju E, Allen EA, Belger A, Ford JM, McEwen S, Mathalon D, Mueller B, Pearlson G, Potkin S, Preda A. 2014. Dynamic functional connectivity analysis reveals transient states of dysconnectivity in schizophrenia. *NeuroImage: Clinical* **5**:298–308 DOI 10.1016/j.nicl.2014.07.003.

Dawson G, Rieder AD, Johnson MH. 2023. Prediction of autism in infants: progress and challenges. *The Lancet Neurology* **22**:244–254 DOI 10.1016/S1474-4422(22)00407-0.

Farah MB, Guesmi R, Kachouri A, Samet M. 2020. A novel chaos based optical image encryption using fractional Fourier transform and DNA sequence operation. *Optics & Laser Technology* **121**:105777 DOI 10.1016/j.optlastec.2019.105777.

Gao C, Zhang X, Wang H, Song L, Hu B, Wang Q. 2022. Two-directional two-dimensional PCA: an efficient face recognition method for thermal infrared images. In: *2022 5th international conference on information communication and signal processing (ICICSP)*. Piscataway: IEEE, 185–191.

Grandjean J, Desrosiers-Gregoire G, Anckaerts C, Angeles-Valdez D, Ayad F, Barrière DA, Blockx I, Bortel A, Broadwater M, Cardoso BM. 2023. A consensus protocol for functional connectivity analysis in the rat brain. *Nature Neuroscience* **26**:673–681 DOI 10.1038/s41593-023-01286-8.

Holz NE, Berhe O, Sacu S, Schwarz E, Tesarz J, Heim CM, Tost H. 2023. Early social adversity, altered brain functional connectivity, and mental health. *Biological Psychiatry* **93**:430–441 DOI 10.1016/j.biopsych.2022.10.019.

Huber L, Finn ES, Chai Y, Goebel R, Stirnberg R, Stöcker T, Marrett S, Uludag K, Kim S-G, Han S. 2021. Layer-dependent functional connectivity methods. *Progress in Neurobiology* **207**:101835 DOI 10.1016/j.pneurobio.2020.101835.

Hutchison RM, Womelsdorf T, Allen EA, Bandettini PA, Calhoun VD, Corbetta M, Della Penna S, Duyn JH, Glover GH, Gonzalez-Castillo J. 2013. Dynamic functional connectivity: promise, issues, and interpretations. *NeuroImage* **80**:360–378 DOI 10.1016/j.neuroimage.2013.05.079.

Kazeminejad A, Sotero RC. 2019. Topological properties of resting-state fMRI functional networks improve machine learning-based autism classification. *Frontiers in Neuroscience* **12**:1018 DOI 10.3389/fnins.2018.01018.

Kumar BV, Aravind R. 2010. Computationally efficient algorithm for face super-resolution using (2D) 2-PCA based prior. *IET Image Processing* **4**:61–69 DOI 10.1049/iet-ipr.2009.0072.

Ladwig Z, Seitzman BA, Dworetsky A, Yu Y, Adeyemo B, Smith DM, Petersen SE, Gratton C. 2022. BOLD cofluctuation 'events' are predicted from static functional connectivity. *NeuroImage* **260**:119476 DOI 10.1016/j.neuroimage.2022.119476.

Lawrence KE, Hernandez LM, Bowman HC, Padgaonkar NT, Fuster E, Jack A, Aylward E, Gaab N, Van Horn JD, Bernier RA. 2020. Sex differences in functional connectivity of the salience, default mode, and central executive networks in youth with ASD. *Cerebral Cortex* **30**:5107–5120 DOI 10.1093/cercor/bhaa105.

Li Y, Liu J, Tang Z, Lei B. 2020. Deep spatial–temporal feature fusion from adaptive dynamic functional connectivity for MCI identification. *IEEE Transactions on Medical Imaging* **39**:2818–2830 DOI 10.1109/TMI.2020.2976825.

Liu J, Sheng Y, Lan W, Guo R, Wang Y, Wang J. 2020. Improved ASD classification using dynamic functional connectivity and multi-task feature selection. *Pattern Recognition Letters* **138**:82–87 DOI 10.1016/j.patrec.2020.07.005.

Liu Y-Y, Li L, Zhang W-H, Chan P-W, Liu Y-S. 2019. Rapid identification of rainstorm disaster risks based on an artificial intelligence technology using the 2DPCA method. *Atmospheric Research* **227**:157–164 DOI 10.1016/j.atmosres.2019.05.006.

Long Y, Cao H, Yan C, Chen X, Li L, Castellanos FX, Bai T, Bo Q, Chen G, Chen N. 2020. Altered resting-state dynamic functional brain networks in major depressive disorder: findings from the REST-meta-MDD consortium. *NeuroImage: Clinical* **26**:102163 DOI 10.1016/j.nicl.2020.102163.

Lu H, Gu Z, Xing W, Han S, Wu J, Zhou H, Ding J, Zhang J. 2019. Alterations of default mode functional connectivity in individuals with end-stage renal disease and mild cognitive impairment. *BMC Nephrology* **20**:1–8 DOI 10.1186/s12882-018-1181-1.

Lurie DJ, Kessler D, Bassett DS, Betzel RF, Breakspear M, Kheilholz S, Kucyi A, Liégeois R, Lindquist MA, McIntosh AR. 2020. Questions and controversies in the study of time-varying functional connectivity in resting fMRI. *Network Neuroscience* **4**:30–69 DOI 10.1162/netn_a_00116.

Matson JL, Nebel-Schwalm M. 2007. Assessing challenging behaviors in children with autism spectrum disorders: a review. *Research in Developmental Disabilities* **28**:567–579 DOI 10.1016/j.ridd.2006.08.001.

Ni L, Wen J, Zhang LJ, Zhu T, Qi R, Xu Q, Liang X, Zhong J, Zheng G, Lu GM. 2014. Aberrant default-mode functional connectivity in patients with end-stage renal disease: a resting-state functional MR imaging study. *Radiology* **271**:543–552 DOI 10.1148/radiol.13130816.

Olczyk P, Kusztal M, Gołębiowski T, Letachowicz K, Krajewska M. 2022. Cognitive impairment in end stage renal disease patients undergoing hemodialysis: markers and risk factors. *International Journal of Environmental Research and Public Health* **19**:2389 DOI 10.3390/ijerph19042389.

Pang X, Liang X, Zhao J, Wu P, Li X, Wei W, Nie L, Chang W, Lv Z, Zheng J. 2022. Abnormal static and dynamic functional connectivity in left and right temporal lobe epilepsy. *Frontiers in Neuroscience* **15**:820641 DOI 10.3389/fnins.2021.820641.

Park BS, Seong M, Ko J, Park SH, Kim YW, wan Kim IH, Park JH, Lee YJ, Park S, Park KM. 2020. Differences of connectivity between ESRD patients with PD and HD. *Brain and Behavior* **10**:e01708 DOI 10.1002/brb3.1708.

Qiu Y, Lv X, Su H, Jiang G, Li C, Tian J. 2014. Structural and functional brain alterations in end stage renal disease patients on routine hemodialysis: a voxel-based morphometry and resting state functional connectivity study. *PLOS ONE* **9**:e98346 DOI 10.1371/journal.pone.0098346.

Razzak I, Saris RA, Blumenstein M, Xu G. 2020. Integrating joint feature selection into subspace learning: a formulation of 2DPCA for outliers robust feature selection. *Neural Networks* **121**:441–451 DOI 10.1016/j.neunet.2019.08.030.

Ricaud B, Borgnat P, Tremblay N, Gonçalves P, Vandergheynst P. 2019. Fourier could be a data scientist: from graph Fourier transform to signal processing on graphs. *Comptes Rendus Physique* **20**:474–488 DOI 10.1016/j.crhy.2019.08.003.

Royer J, Bernhardt BC, Larivière S, Gleichgerrcht E, Vorderwülbecke BJ, Vulliémoz S, Bonilha L. 2022. Epilepsy and brain network hubs. *Epilepsia* **63**:537–550 DOI 10.1111/epi.17171.

Sadat A, Joye IJ. 2020. Peak fitting applied to fourier transform infrared and raman spectroscopic analysis of proteins. *Applied Sciences* **10**:5918 DOI 10.3390/app10175918.

Shen M, Wen P, Song B, Li Y. 2023. Automatic identification of schizophrenia based on EEG signals using dynamic functional connectivity analysis and 3D convolutional neural network. *Computers in Biology and Medicine* **160**:107022 DOI 10.1016/j.compbiomed.2023.107022.

Shi Y, Tong C, Zhang M, Gao X. 2019. Altered functional connectivity density in the brains of hemodialysis end-stage renal disease patients: an in vivo resting-state functional MRI study. *PLOS ONE* **14**:e0227123 DOI 10.1371/journal.pone.0227123.

Starck T, Nikkinen J, Rahko J, Remes J, Hurtig T, Haapsamo H, Jussila K, Kuusikko-Gauffin S, Mattila M-L, Jansson-Verkasalo E. 2013. Resting state fMRI reveals a default mode dissociation between retrosplenial and medial prefrontal subnetworks in ASD despite motion scrubbing. *Frontiers in Human Neuroscience* **7**:802.

Sun J, Zhao R, He Z, Chang M, Wang F, Wei W, Zhang X, Zhu Y, Xi Y, Yang X. 2022. Abnormal dynamic functional connectivity after sleep deprivation

from temporal variability perspective. *Human Brain Mapping* **43**:3824–3839 DOI 10.1002/hbm.25886.

Sun Y, Collinson SL, Suckling J, Sim K. 2019. Dynamic reorganization of functional connectivity reveals abnormal temporal efficiency in schizophrenia. *Schizophrenia Bulletin* **45**:659–669 DOI 10.1093/schbul/sby077.

Valentine ML, Al-Mualem ZA, Baiz CR. 2021. Pump slice amplitudes: a simple and robust method for connecting two-dimensional infrared and Fourier transform infrared spectra. *The Journal of Physical Chemistry A* **125**:6498–6504 DOI 10.1021/acs.jpca.1c04558.

Valsasina P, Hidalgodela Cruz M, Filippi M, Rocca MA. 2019. Characterizing rapid fluctuations of resting state functional connectivity in demyelinating, neurodegenerative, and psychiatric conditions: from static to time-varying analysis. *Frontiers in Neuroscience* **13**:618 DOI 10.3389/fnins.2019.00618.

Van Den Heuvel MP, Pol HEH. 2010. Exploring the brain network: a review on resting-state fMRI functional connectivity. *European Neuropsychopharmacology* **20**:519–534 DOI 10.1016/j.euroneuro.2010.03.008.

Wang G, Zhang L, Qiao L. 2023. The effect of node features on GCN-based brain network classification: an empirical study. *PeerJ* **11**:e14835 DOI 10.7717/peerj.14835.

Wang X, Wang J, Yan K. 2018. Gait recognition based on Gabor wavelets and (2D) 2 PCA. *Multimedia Tools and Applications* **77**:12545–12561 DOI 10.1007/s11042-017-4903-7.

Wee C-Y, Yang S, Yap P-T, Shen D, Initiative AsDN. 2016. Sparse temporally dynamic resting-state functional connectivity networks for early MCI identification. *Brain Imaging and Behavior* **10**:342–356 DOI 10.1007/s11682-015-9408-2.

Xu S, Li M, Yang C, Fang X, Ye M, Wei L, Liu J, Li B, Gan Y, Yang B. 2019. Altered functional connectivity in children with low-function autism spectrum disorders. *Frontiers in Neuroscience* **13**:806 DOI 10.3389/fnins.2019.00806.

Yang Z, Wen M, Wei Y, Huang H, Zheng R, Wang W, Gao X, Zhang M, Cheng J, Han S. 2022. Alternations in dynamic and static functional connectivity density in chronic smokers. *Frontiers in Psychiatry* **13**:843254 DOI 10.3389/fpsyt.2022.843254.

Yao S, Becker B, Kendrick KM. 2021. Reduced inter-hemispheric resting state functional connectivity and its association with social deficits in autism. *Frontiers in Psychiatry* **12**:629870 DOI 10.3389/fpsyt.2021.629870.

Ye H, Robak LA, Yu M, Cykowski M, Shulman JM. 2023. Genetics and pathogenesis of Parkinson's syndrome. *Annual Review of Pathology: Mechanisms of Disease* **18**:95–121 DOI 10.1146/annurev-pathmechdis-031521-034145.

Yu S-S, Zhou N-R, Gong L-H, Nie Z. 2020. Optical image encryption algorithm based on phase-truncated short-time fractional Fourier transform and hyper-chaotic system. *Optics and Lasers in Engineering* **124**:105816 DOI 10.1016/j.optlaseng.2019.105816.

Zhang D, Wang Y, Zhou L, Yuan H, Shen D, Initiative AsDN. 2011. Multimodal classification of Alzheimer's disease and mild cognitive impairment. *NeuroImage* **55**:856–867 DOI 10.1016/j.neuroimage.2011.01.008.

Zhang J, Small M. 2006. Complex network from pseudoperiodic time series: topology versus dynamics. *Physical Review Letters* **96**:238701 DOI 10.1103/PhysRevLett.96.238701.

Zhao F, Chen Z, Rekik I, Lee S-W, Shen D. 2020. Diagnosis of autism spectrum disorder using central-moment features from low-and high-order dynamic resting-state functional connectivity networks. *Frontiers in Neuroscience* **14**:258 DOI 10.3389/fnins.2020.00258.

Zhou G, Xu G, Hao J, Chen S, Xu J, Zheng X. 2019. Generalized centered 2-D principal component analysis. *IEEE Transactions on Cybernetics* **51**:1666–1677.

Zou Y, Tang W, Qiao X, Li J. 2021. Aberrant modulations of static functional connectivity and dynamic functional network connectivity in chronic migraine. *Quantitative Imaging in Medicine and Surgery* **11**:2253 DOI 10.21037/qims-20-588.